Silicon Slot Waveguides With Low Transmission and Bending Losses at 1064 nm

Xiangdong Li, Xue Feng, Xian Xiao, Yihang Li, Kaiyu Cui, Fang Liu, and Yidong Huang, *Member, IEEE*

***Abstract*— Silicon slot waveguides operating at a wavelength of high silicon absorption are fabricated on silicon-on-insulator wafers. The measured transmission loss coefficient is as low as 6∼8 dB/cm at 1064 nm, which is much lower than the material absorption. In addition, the bending loss of the slot waveguides is measured as 4.1∼4.6 dB/180° with a bending radius of 15 μm. Both the transmission and bending losses are analyzed and discussed. We believe that this work could pave the way to achieve all-silicon photonic integrated circuits, which are very promising for a future on-chip chemical/biological analysis.**

***Index Terms*— Photonic integrated circuit, slot waveguide, transmission loss, bending loss, high absorption.**

I. Introduction

SILICON photonic integrated circuits (PICs) have attracted much interest due to the possibility of merging electronics and photonics monolithically [1]–[3]. Silicon photodetectors are readily realized through implementing p-n junctions. Silicon emitters have come a long way for emitting within the wavelength of 800 nm - 1100 nm [4]–[6]. Thus, it is possible to achieve all-silicon PICs with mature and cost-effective complementary metal-oxide-semiconductor (CMOS) fabrication process [7]. Furthermore, silicon PICs also provide a versatile platform for chemical and biological analysis [8]–[10]. Specifically, the wavelength window (750 nm to 1200 nm) for optical trapping of biological cells and small organisms [11] is fortunately falling into the operational wavelength band of silicon emitters. Additionally, the shortwave near-infrared (SW-NIR) wavelengths could also be adopted for in-vivo imaging [12]. However, for a PIC with silicon emitters and photodetectors, the transmission line would be a major challenge since the emission from silicon emitters would be highly absorbed by silicon wire waveguides [13]. In [14] and [15], we have proposed and demonstrated that slot waveguides are promising to reduce the transmission loss due to material absorption since the light is confined within the slot region [16], [17]. Besides the low transmission loss, the slot region could also provide a useful channel for interaction between the filler and the light [18] or optical manipulation [19], which is desired in chemical and biological analysis. Thus, silicon slot waveguides may provide a possible solution for the transmission line in all-silicon PICs.

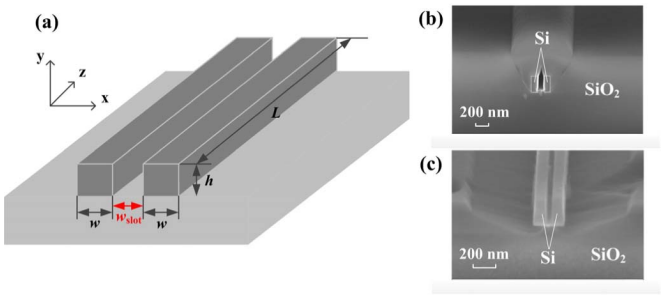

Fig. 1. (a) Schematic of the silicon slot waveguide without a silica cladding layer. (b) SEM image of the slot waveguide after PECVD with $w_{slot} = 60$ nm. (c) SEM image of the slot waveguide without a clading layer with $w_{slot} = 60$ nm.

In this work, after optimizing the fabrication process, we have experimentally investigated the transmission and bending losses of slot waveguides fabricated on silicon-on-insulator (SOI) wafers. For straight waveguides, the measured transmission loss coefficient at the wavelength of 1064 nm could be as low as 5.98 ± 0.45 dB/cm and 7.97 ± 1.56 dB/cm with the slot width of 120 nm and 60 nm, respectively. Such values are much lower than the silicon absorption (50 dB/cm @ 1064 nm). For bending slot waveguides with a radius of 15 μm, the measured values of bending loss are 4.09 ± 0.40 dB/180° and 4.59 ± 0.55 dB/180° for the samples with a slot width of 120 nm and 60 nm, respectively. Furthermore, we have also analyzed and discussed the impact of structural parameters and fabrication process on the transmission and bending losses.

II. Principle, Design and Fabrication

Figure 1(a) depicts the schematic of a silicon slot waveguide. The width of the total waveguide w_{total} can be determined by $w_{total} = w_{slot} + 2 \times w$, where w_{slot} and w are the widths of the slot region and the silicon strips, respectively. We have adopted w as 90 nm with w_{slot} of 120 nm and 60 nm. All waveguides are fabricated on SOI wafers, in which the thickness of the top silicon layer is $h = 220$ nm and that of the buried oxide layer is 3 μm. The pattern is defined with electron beam lithography (EBL). All the waveguides are etched

Manuscript received May 25, 2015; revised August 27, 2015; accepted September 11, 2015. Date of publication September 22, 2015; date of current version November 23, 2015. This work was supported in part by the National Basic Research Program of China under Grant 2011CBA00608 and Grant 2011CBA00303, and in part by the National Natural Science Foundation of China under Grant 61036011 and Grant 61036010. *(Corresponding author: Xue Feng.)*

The authors are with the Tsinghua National Laboratory for Information Science and Technology, Department of Electronic Engineering, Tsinghua University, Beijing 100084, China (e-mail: lixiangdong11@mails.tsinghua.edu.cn; x-feng@tsinghua.edu.cn; xiaox12@mails.tsinghua.edu.cn; li.yihang@wustl.edu; kaiyucui@tsinghua.edu.cn; liu_fang@tsinghua.edu.cn; yidonghuang@tsinghua.edu.cn).

Color versions of one or more of the figures in this letter are available online at http://ieeexplore.ieee.org.

Digital Object Identifier 10.1109/LPT.2015.2478900

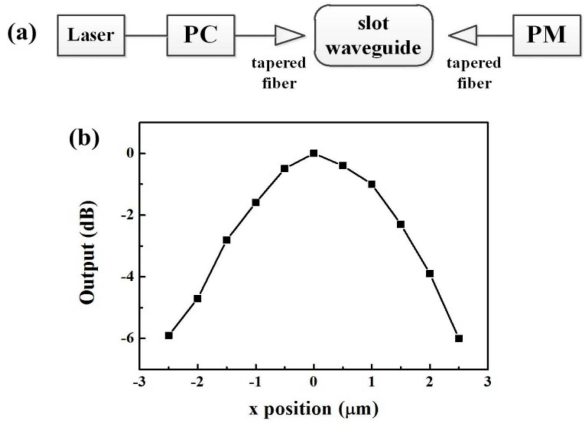

Fig. 2. (a) Schematic of the measurement system. (b) Normalized output under different input positions.

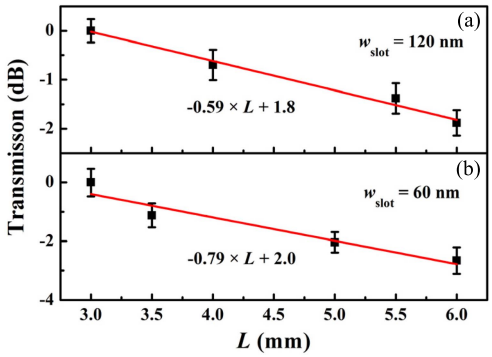

Fig. 3. Measured transmission losses of slot waveguides for (a) $w_{\text{slot}} = 120$ nm and (b) $w_{\text{slot}} = 60$ nm, respectively.

by inductively coupled plasma reactive ion etch (ICP-RIE) with the gases of SF_6 and O_2. In [14], the transmission loss coefficient of silicon slot waveguides was measured to be as high as $\sim$ 23 dB/cm at the operating wavelength of $\lambda = 1064$ nm, which is mainly due to the scattering loss caused by the surface roughness of sidewalls. In this work, the operating wavelength is still 1064 nm but the etching parameters in terms of gas flow, gas pressure and etching power are optimized to improve etching quality of waveguides, especially the sidewall roughness. After etching, the silicon waveguides are covered by a SiO_2 cladding layer with a thickness of 600 nm through plasma enhanced chemical vapor deposition (PECVD) with SiH_4 and N_2O. Here, the cladding layer is adopted to protect the silicon slot waveguide since lapping, grinding and polishing are needed in our fabrication process, which is the same as in [14]. The photographs of scanning electron microscopy (SEM) for the slot waveguide ($w_{\text{slot}} = 60$ nm) with and without the cladding layer are shown in Figs. 1(b) and (c), respectively.

The samples are characterized with a measurement system as shown in Fig. 2(a), including a 1064 nm laser, a polarization controller (PC, Agilent 11896A), and a power meter (PM, Agilent 81624A). Two single-mode lensed optical fibers with a spot radius of about 2 μm, which are separately mounted on a computer-controlled alignment stage, are used to couple light in and out of the slot waveguides directly. The output power of the laser is set as a constant value of 1 mW (0 dBm). Only the transverse-electric (TE) polarization is measured since the loss of the transverse-magnetic (TM) mode is much higher than that of the TE mode [14]. In order to ensure the light transmits through the slot waveguide, the output power under different positions of both the input and output lensed fibers along the x-axis has been measured for each sample. For simplicity, only a typical output with varied positions of the input lensed fiber is shown in Fig. 2(b). The point of 0 μm represents the origin position after alignment and the power is also normalized with the maximum value, which indicates that the light is coupled into the slot waveguide.

By subtracting the output power of the system from the laser output, we obtain the total transmission loss of the system, which is the sum of the insertion loss of PC, the coupling loss between the tapered fiber and the waveguide, and the transmission loss of the slot waveguide. In order to extract the transmission loss of slot waveguide, samples with varied length (from 3 mm to 6 mm) for each w_{slot} are prepared. Here, all waveguides with different lengths are fabricated on the same chip, while the waveguide length is determined by the mask layout with the same bending (the radius is 10 μm) and different straight lengths. Thus, the transmission loss coefficient could be revealed by linear fitting the measured transmission losses among the waveguides with different lengths. Since all waveguides are fabricated on the same chip, the surface roughness is supposed to be similar. Furthermore, for each pair of w_{slot} and waveguide length (L), there are five samples so that the fluctuation of coupling loss could be averaged by measuring all the five samples.

III. Measurements, Results and Analysis

In Figs. 3(a) and (b), the measured losses of waveguides are shown as functions of L for two cases, $w_{\text{slot}} = 120$ and 60 nm, respectively. For each curve, the data are normalized to the transmission loss of the waveguide with a length of 3 mm. In Fig. 3, each data point and error bar represents the average loss and the standard deviation, respectively. The standard deviation is 0.24 dB $\sim$ 0.47 dB, which may be introduced by the varied coupling. The red solid lines are the linear fitting results, and the slope represents the transmission loss coefficient, which is 5.98 $\pm$ 0.45 dB/cm and 7.97 $\pm$ 1.56 dB/cm for w_{slot}120 nm and 60 nm, respectively. Both of them are much lower than the material absorption of silicon (50 dB/cm @ 1064 nm), which indicates that silicon slot waveguides could be applied to transmit light within the high silicon absorption band. For example, if the total transmission loss of PICs should be less than 10 dB, the transmission distance of our samples could be more than 1 cm (1.2 cm $\sim$ 1.5 cm).

In order to attain insights of the loss mechanism, we have carried out some numerical simulations and calculations. First, the absorption loss of slot waveguides due to silicon material is simulated by finite-element method (FEM) as in [15]. The electric-field distributions of TE polarization and the corresponding electric field intensities distributing along the x-axis for slot waveguides with $w_{\text{slot}} = 120$ nm and 60 nm are shown in Fig. 4. According to the scanning electron

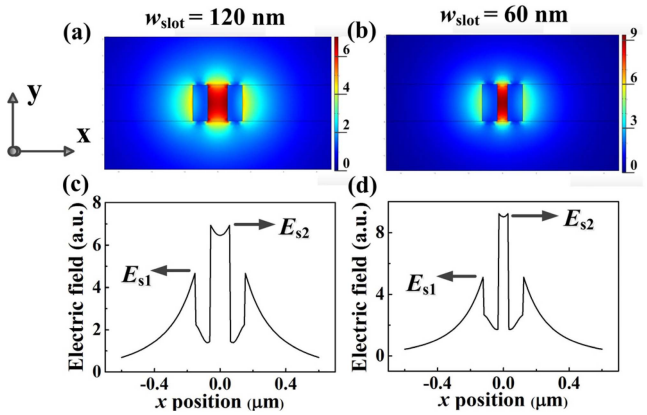

Fig. 4. Simulated profiles of TE polarization for slot waveguides with (a) $w_{slot} = 120$ nm and (b) $w_{slot} = 60$ nm. The corresponding electric field intensity distributing along the x-axis for (c) $w_{slot} = 120$ nm and (d) $w_{slot} = 60$ nm, respectively.

microscope (SEM) photograph shown in Fig. 1(b), the slot waveguide is surrounded by silica but filled with air. Under this condition, the transmission loss coefficients for the two cases are calculated as 0.60 dB/cm and 1.3 dB/cm, respectively. These losses are much lower than our measured results. Thus, the transmission loss is not mainly determined by the material absorption. As discussed in [14], the transmission loss would be introduced by not only absorption loss but also scattering loss. Scattering loss is mainly introduced by the roughness of the etched sidewalls. There are some reports about the three-dimensional accurate modeling of scattering loss [20], [21]. Here, in order to obtain some clear and simple guidelines for practical fabrications, the scattering loss is approximately estimated with a simple analytical formula as in [22] and [23]:

$$\alpha = \frac{\sigma^2 k_0^2 h}{\beta} \cdot \frac{E_s^2}{\int E^2 dx} \cdot \Delta n^2 \tag{1}$$

where σ is the standard deviation of interface roughness, k_0 is the free-space wave number, Δn is the difference between the refractive indices of the core and the cladding, β is the modal propagation constant, h is the transverse propagation constant, while $E_s^2 / \int E^2 dx$ is the normalized electric field intensity at the interface. From the SEM image shown in Fig. 1(c), the amplitude of the surface roughness at etched sidewalls of our fabricated samples is about 5 nm. Following the result shown in [23], we estimate $\sigma \sim 2$ nm. The electric field intensities distributing along the x-axis for $w_{slot} = 120$ nm/60 nm are shown in Fig. 4(c)/(d).

Here, E_{s2} and E_{s1} represent the maxima of the electric field intensities on the strip waveguide inner and outer sidewalls, respectively. The values of E_{s2}/E_{s1} are about 1.4 and 1.9 for the two structures. This indicates that the light confinement in the slot region is more pronounced as w_{slot} is narrowed, while the scattering loss is also higher according to Eq. (1). The scattering loss coefficients could be estimated as 4.7 dB/cm and 5.9 dB/cm for $w_{slot} = 120$ nm and 60 nm, respectively. Thus, the total transmission losses, including material absorption and sidewall scattering, can be estimated as 5.3 dB/cm and 7.2 dB/cm for $w_{slot} = 120$ nm and 60 nm, respectively. These values are very close to the experimental results of 5.98 dB/cm and 7.97 dB/cm. According to the aforementioned calculations, the transmission loss in this work is improved mainly by reducing the sidewall roughness but the scattering loss is still dominant. Thus, there is still some room to further improve the transmission loss. Additionally, it should be mentioned that the structural parameters are not the optimal ones according to our simulation [15]. Taking $w_{total} = 300$ nm as an example, the optimal structural parameters are $w = 60$ nm and $w_{slot} = 140$ nm, while the transmission loss coefficient (without scattering loss) is ~ 0.4 dB/cm, which is only slightly lower than that in this work (~ 0.60 dB/cm at $w = 90$ nm and $w_{slot} = 120$ nm). However, such an optimized structure is more difficult to fabricate ($w = 60$ nm vs. $w = 90$ nm), while the improvement is limited (~ 0.4 dB/cm vs. ~ 0.6 dB/cm). Thus, we believe that it would be more valuable to reduce the sidewall roughness so that better transmission loss coefficient can be achieved.

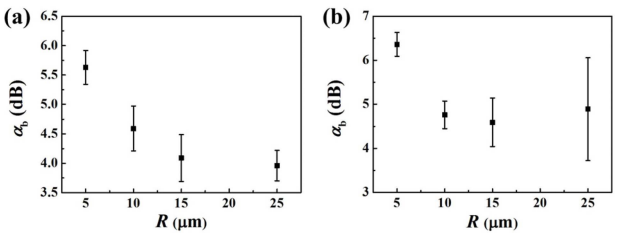

Fig. 5. Measured bending loss (per 180°) for different bending radii with (a) $w_{slot} = 120$ nm and (b) $w_{slot} = 60$ nm.

For a practical PIC, bending waveguide is also desired. Thus, the bending loss (α_b) of silicon slot waveguides has also been investigated at wavelength of 1064 nm. In experiments, several samples with a varied bending radius (R) of 5 μm, 10 μm, 15 μm, and 25 μm are fabricated. For each sample, the length along the z-axis is 3 mm and the bending angles are all 180°. On the same wafer, the straight slot waveguides with a length of 3 mm are also fabricated as reference. There are three samples for each bending radius, while there are five for each straight waveguide, with $w_{slot} = 120$ nm and 60 nm. Thus, the bending loss could be determined by subtracting the transmission loss of straight slot waveguides from that with a bending slot waveguide. Figure 5 shows the bending loss (per 180°) would decrease as the radius increases and is nearly constant after the radius is larger than 15 μm. The values at $R = 15$ μm are 4.09 ± 0.40 dB/180° and 4.59 ± 0.55 dB/180° for $w_{slot} = 120$ nm and 60 nm, respectively. It should be noted that the variation for $w_{slot} = 60$ nm and $R = 25$ μm is larger than those of other cases, which may be originated from the fabrication errors.

Moreover, we have performed simulations to attain insights of the bending loss mechanism. The results are shown in Fig. 6. As the bending radius increases from $R = 5$ μm to 25 μm, the loss would decrease from several dB to $\sim$1 dB. Specifically, when $R = 5$ μm, the calculated bending loss is as high as about 3.8 dB and 5.6 dB for $w_{slot} = 120$ nm and $w_{slot} = 60$ nm, respectively. At a small bending radius, a high bending loss is mainly because the light field would tend to distribute into the lateral sidewall as shown in the left inset in Fig. 6 ($w_{slot} = 120$ nm and $R = 5$ μm).

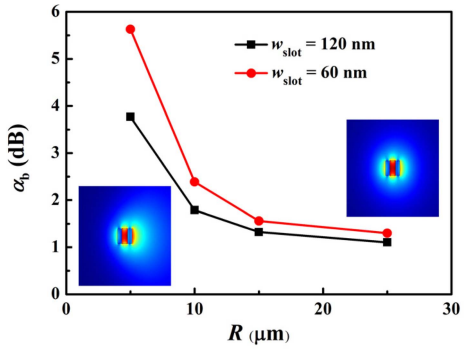

Fig. 6. Simulated bending losses (per 180° for different bending radii with $w_{slot} = 120$ nm (black squares) and $w_{slot} = 60$ nm (red circles). The left and right insets are the electric field distributions of TE polarization for $w_{slot} = 120$ nm at $R = 5$ μm and at $R = 25$ μm, respectively.

Thus, some energy would be transferred to radiation modes, while the propagation mode would experience more absorption due to the silicon strip. However, as the bending radius increases, the asymmetry of the propagation mode would be reduced as shown in the right inset in Fig. 6 ($w_{slot} = 120$ nm and $R = 25$ μm) so that the bending loss could be lower. Comparing the results shown in Fig. 5 and Fig. 6, we find that the variation trend of the measured bending loss with bending radius is quite similar to the simulated result, except the measured loss exceeds the calculated one. But the measured loss is higher than the calculated one. The reason is that the calculated bending loss only includes absorption loss and radiation loss but without scattering loss. Actually, it is very hard to calculate the scattering loss despite of the analytical and numerical methods. Although the calculated value is not consistent with that measured in experiments, it also provides some useful guidelines. With the comparison between the calculated and measured values, we believe that the bending loss could be improved by reducing the fabrication error and the sidewall roughness as discussed for the straight waveguides. Besides improving the fabrication process, another possible way to reduce the bending loss is to introduce asymmetrical slot waveguide [24] and the related work is still ongoing.

IV. Conclusions

In conclusion, silicon slot waveguides are fabricated on SOI wafers and both the transmission loss and the bending loss are experimentally investigated at the wavelength of 1064 nm. The measured transmission loss coefficients for $w_{slot} = 120$ nm and 60 nm could be as low as 5.98 ± 0.45 dB/cm and 7.97 ± 1.56 dB/cm, respectively. The bending loss at $R = 15$ μm is 4.09 ± 0.40 dB/180° and 4.59 ± 0.55 dB/180° for $w_{slot} = 120$ nm and 60 nm, respectively. Furthermore, we have calculated the absorption loss and estimated the scattering loss of our fabricated slot waveguides. The result indicates that the measured transmission loss is mainly due to scattering by the surface irregularities. The mechanism of bending loss is also discussed and the possible way to improve it is also discussed. All in all, we believe that silicon slot waveguides provide a possible solution to realize all-silicon PICs for on-chip chemical/biological analysis.

Acknowledgment

The authors would like to thank Dr. Wei Zhang, Dr. Dengke Zhang, Dr. Yongzhuo Li and Mr. Feng Zhu for their valuable discussions and helpful comments.

References

[1] B. Jalali and S. Fathpour, "Silicon photonics," *J. Lightw. Technol.*, vol. 24, no. 12, pp. 4600–4615, Dec. 2006.
[2] N. Daldosso and L. Pavesi, "Nanosilicon photonics," *Laser Photon. Rev.*, vol. 3, no. 6, pp. 508–534, Nov. 2009.
[3] R. Soref, "The past, present, and future of silicon photonics," *IEEE J. Sel. Topics Quantum Electron.*, vol. 12, no. 6, pp. 1678–1687, Nov./Dec. 2006.
[4] D. Liang and J. E. Bowers, "Recent progress in lasers on silicon," *Nature Photon.*, vol. 4, no. 8, pp. 511–517, Aug. 2010.
[5] K.-Y. Cheng, R. Anthony, U. R. Kortshagen, and R. J. Holmes, "High-efficiency silicon nanocrystal light-emitting devices," *Nano Lett.*, vol. 11, no. 5, pp. 1952–1956, Apr. 2011.
[6] M. A. Green, J. Zhao, A. Wang, P. J. Reece, and M. Gal, "Efficient silicon light-emitting diodes," *Nature*, vol. 412, no. 23, pp. 805–808, Aug. 2001.
[7] S.-I. Saito *et al.*, "Silicon light-emitting transistor for on-chip optical interconnection," *Appl. Phys. Lett.*, vol. 89, no. 16, pp. 163504-1–163504-3, Oct. 2006.
[8] H. Schmidt and A. R. Hawkins, "The photonic integration of non-solid media using optofluidics," *Nature Photon.*, vol. 5, no. 10, pp. 598–604, Oct. 2011.
[9] X. Fan and I. M. White, "Optofluidic microsystems for chemical and biological analysis," *Nature Photon.*, vol. 5, no. 10, pp. 591–597, Oct. 2011.
[10] F. Dell'Olio and V. M. N. Passaro, "Optical sensing by optimized silicon slot waveguides," *Opt. Exp.*, vol. 15, no. 8, pp. 4977–4993, Apr. 2007.
[11] K. C. Neuman and S. M. Block, "Optical trapping," *Rev. Sci. Instrum.*, vol. 75, no. 9, pp. 2787–2809, Sep. 2004.
[12] R. Weissleder, "A clearer vision for *in vivo* imaging," *Nature Biotechnol.*, vol. 19, no. 4, pp. 316–317, Apr. 2001.
[13] E. D. Palik, *Handbook of Optical Constants of Solids*. San Diego, CA, USA: Harcourt Brace Jovanovich, 1985.
[14] X. Li, X. Feng, X. Xiao, K. Cui, F. Liu, and Y. Huang, "Experimental demonstration of silicon slot waveguide with low transmission loss at 1064 nm," *Opt. Commun.*, vol. 329, pp. 168–172, Oct. 2014.
[15] X. Li, X. Feng, K. Cui, F. Liu, and Y. Huang, "Designing low transmission loss silicon slot waveguide at wavelength band of high material absorption," *Opt. Commun.*, vol. 306, pp. 131–134, Oct. 2013.
[16] V. R. Almeida, Q. Xu, C. A. Barrios, and M. Lipson, "Guiding and confining light in void nanostructure," *Opt. Lett.*, vol. 29, no. 11, pp. 1209–1211, Jun. 2004.
[17] Q. Xu, V. R. Almeida, R. R. Panepucci, and M. Lipson, "Experimental demonstration of guiding and confining light in nanometer-size low-refractive-index material," *Opt. Lett.*, vol. 29, no. 14, pp. 1626–1628, Jul. 2004.
[18] M. P. Hiscocks, C.-H. Su, B. C. Gibson, A. D. Greentree, L. C. L. Hollenberg, and F. Ladouceur, "Slot-waveguide cavities for optical quantum information applications," *Opt. Exp.*, vol. 17, no. 9, pp. 7295–7303, Apr. 2009.
[19] A. H. J. Yang, S. D. Moore, B. S. Schmidt, M. Klug, M. Lipson, and D. Erickson, "Optical manipulation of nanoparticles and biomolecules in sub-wavelength slot waveguides," *Nature*, vol. 457, no. 7225, pp. 71–75, Jan. 2009.
[20] T. Barwicz and H. A. Haus, "Three-dimensional analysis of scattering losses due to sidewall roughness in microphotonic waveguides," *J. Lightw. Technol.*, vol. 23, no. 9, pp. 2719–2732, Sep. 2005.
[21] C. Ciminelli, F. Dell'Olio, V. M. N. Passaro, and M. N. Armenise, "Fully three-dimensional accurate modeling of scattering loss in optical waveguides," *Opt. Quantum Electron.*, vol. 41, no. 4, pp. 285–298, Mar. 2009.
[22] P. K. Tien, "Light waves in thin films and integrated optics," *Appl. Opt.*, vol. 10, no. 11, pp. 2395–2413, Nov. 1971.
[23] Y. A. Vlasov and S. J. McNab, "Losses in single-mode silicon-on-insulator strip waveguides and bends," *Opt. Exp.*, vol. 12, no. 8, pp. 1622–1631, Apr. 2004.
[24] P. A. Anderson, B. S. Schmidt, and M. Lipson, "High confinement in silicon slot waveguides with sharp bends," *Opt. Exp.*, vol. 14, no. 20, pp. 9197–9202, Oct. 2006.